AIMS Mathematics, 10(8): 17998–18023.
DOI: 10.3934/math.2025802
Received: 12 May 2025
Revised: 29 July 2025
Accepted: 01 August 2025
Published: 08 August 2025

https://www.aimspress.com/journal/Math

Research article

Dynamics of a discrete-time prey-predator system with nonstandard finite difference scheme

Özlem Ak Gümüş*

Adıyaman University, Faculty of Arts and Sciences, Department of Mathematics, 02040, Adıyaman, Turkey

* **Correspondence:** E-mail: akgumus@adiyaman.edu.tr.

Abstract: This study investigates the stability and bifurcation analysis of a discrete-time predator-prey system using a nonstandard finite difference scheme. We analytically demonstrate that the system undergoes a Neimark–Sacker bifurcation near its unique positive fixed point. To suppress the resulting chaotic dynamics, control strategies based on the OGY and state feedback control methods are implemented. Numerical simulations are conducted to support the theoretical analysis, confirming the effectiveness of the proposed control techniques.

Keywords: NSFD; prey-predator system; stability; bifurcation theory; chaos control
Mathematics Subject Classification: 39A30, 92D25, 93C55, 34C23, 37N25

1. Introduction

Predator-prey interactions play a crucial role in maintaining ecosystem stability; therefore, investigating the dynamics of predator and prey populations is of great importance in population ecology [1, 2]. In predator-prey populations, which generally exhibit complex dynamics, decision-making processes are essential to maintain ecological balance. For this purpose, many researchers have investigated discrete-time predator-prey models from multiple perspectives: In [3], the effect of prey migration is analyzed and a feedback-based chaos control strategy is implemented. The role of the Allee effect is investigated in [4], where it is shown that the emergence of flip and Neimark–Sacker bifurcations leads to chaotic behavior, which is effectively controlled using both the OGY method and a hybrid control strategy. In [5], a model based on the time-delay effect is investigated, and it is revealed that delay can destabilize populations and create complex stock patterns. In [6], it is shown that predator harvesting produces rich bifurcation structures, including flip and Neimark–Sacker types. In [7], the study focuses on Allee-induced bifurcations and successfully applies a state-feedback control method to stabilize the system dynamics. In [8], a model with nonlinear effects of the Allee

mechanism is analyzed, transitions from stability to chaos are demonstrated, and effective control strategies are proposed. In [9], Neimark–Sacker bifurcation with predator harvesting is considered and feedback control is used to reduce instability. In [10], it is shown that torus doubling routes lead to chaos in systems with delays and harvesting is proposed as a method of chaos suppression. In [11], complex dynamics, including chaotic and quasi-periodic behavior, are investigated in systems with strong and weak Allee effects. In [12], the FAST approach is introduced to efficiently determine bifurcation transitions in models with weak Allee effects and feedback control is used to stabilize the chaotic dynamics. Finally, [13] presents a comprehensive theoretical and numerical investigation of multiple bifurcation phenomena, including resonant states, in a model with prey harvesting effort, offering practical insights for ecological management.

The temporal fluctuations in population sizes have led scientists to analyze mathematical models that describe populations, aiming to better understand their life cycles. A thorough understanding of predator-prey dynamics is essential for the development and analysis of mathematical models that accurately capture the behavior of prey and predator populations. Following the Lotka–Volterra [14, 15] models that included non-finite predation, Gauss-type predator-prey models with finite functional responses have been widely investigated [16–18]. Those that include the Michaelis–Menten (Holling type II) functional response constitute the most extensively studied class of predator-prey models [2, 19–22].

Predator-prey interactions are central to ecosystem functioning, regulating population sizes and preventing species extinction due to overpopulation or overexploitation. Classic examples include lynx-hare dynamics in boreal forests or phytoplankton–zooplankton interactions in aquatic systems. These systems often exhibit nonlinear, cyclical, or chaotic behavior due to predation pressure, prey availability, and environmental variability. The proposed model contributes to this body of knowledge by simulating such biological scenarios under a nonstandard finite difference (NSFD) scheme framework, ensuring biological realism, such as positivity and finiteness of solutions. The nonlinear dynamics captured by our model reflect classic predator-prey interactions, such as the lynx-hare cycle observed in boreal forests or phytoplankton–zooplankton systems in aquatic environments. These systems exhibit saturation in predation rates and seasonal breeding patterns, making them well-suited for discrete-time modeling with Holling type II responses. Many studies have analyzed predator-prey models incorporating the Holling type II functional response using NSFD schemes to preserve positivity and fixed-point structure. Examples include [23] and [19], which show that discrete models based on NSFD schemes maintain biological consistency while allowing for rich bifurcation behavior.

Population dynamics can be modeled using either differential equations or difference equations. Discrete-time models, particularly well suited to organisms with non-overlapping generations such as annual insects or some amphibians, often display richer and more intricate behaviors than their continuous-time counterparts by better capturing life cycle transitions [24, 25]. Numerical methods based on finite-difference approximations are advantageous for analyzing the dynamics of interacting population models. NSFD schemes preserve the fundamental structural properties of continuous models, while also ensuring positive solutions under positive initial conditions [26, 27].

The motivation behind this work stems from the need to understand the complex dynamics of interacting prey and predator populations, especially in ecosystems where nonlinear behavior and bifurcations play a critical role. Discrete-time models with NSFD provide a powerful framework to capture these dynamics, especially in species with nonoverlapping generations. This article aims to

provide insights into the emergence of complex states, including chaos, by analyzing the stability and bifurcation structure of such systems, and to explore effective control strategies.

A Lotka–Volterra population model [24] describing predator-prey interactions is defined as follows:

$$\begin{aligned} \dot{x} &= ax - bxy \\ \dot{y} &= \gamma xy - sy \end{aligned} \tag{1.1}$$

where x and y stand for prey and predator populations, respectively, and a, b, s, and γ are positive constants: The natural growth rate of prey, predation rate, the rate of predator death, and the rate at which prey is converted into predators, respectively. Accordingly, model (1.1) is expanded in [28] to the following general form: $\dot{x} = ax - y\psi(x)$ and $\dot{y} = \gamma\psi(x)y - sy$, where $\psi(x)$ is the predator's response function. A generalized predator-prey model has been presented in [29]: $\dot{x} = \omega(x) - y\psi(x)$ and $\dot{y} = \gamma\psi(x)y - sy$, where the logistic growth function is represented by $\omega(x) = r(1 - \frac{x}{k})$ and the Michaelis–Menten type functional responses by $\psi(x) = \frac{ax}{b+x}$. A more advanced form of this model is introduced in [30] by taking $\alpha = \frac{a}{b}$ and $n = \frac{1}{b}$ as follows:

$$\begin{aligned} \dot{x} &= rx(1 - \frac{x}{k}) - \frac{\alpha xy}{1 + nx} \\ \dot{y} &= \frac{\alpha\delta xy}{1 + nx} - ys. \end{aligned} \tag{1.2}$$

In the model, x and y represent the prey and predator populations, respectively, while r, k, s, α, n, and δ are all positive constants. Here, r denotes the intrinsic growth rate of the prey, s is the natural mortality rate of the predator, δ is the efficiency of converting consumed prey into predator biomass, k is carrying capacity, and α is a positive interaction coefficient.

In recent years, the modeling of predator-prey dynamics has evolved to include increasingly realistic ecological factors such as stage structure, time delay, cannibalism, and spatial diffusion. For instance, [31] examined a delayed predator-prey system incorporating stage structure and a square-root functional response, highlighting how time delays can destabilize coexistence and trigger Hopf bifurcations through local stability analysis and normal form techniques. Meanwhile, [32] addressed the role of cannibalism and non-overlapping generations in generating complex codimension-two bifurcation phenomena in discrete-time models. Their findings underscore the influence of internal prey dynamics and resonance effects (e.g., 1:2, 1:3, 1:4) on the emergence of intricate synchronized orbits. In a spatial context, [33] investigated a discrete predator-prey model on a coupled map lattice with diffusion, where Neimark–Sacker and flip bifurcations, along with various Turing instabilities, were explored. These studies collectively emphasize the need for discrete frameworks that preserve key biological features while also capturing spatiotemporal and behavioral feedback mechanisms. Motivated by this body of research, our study contributes to the ongoing effort by formulating a discrete-time predator-prey model based on an NSFD scheme, focusing on controlling chaotic oscillations and ensuring biological realism through structural properties such as positivity, boundedness, and discrete feedback.

The dynamics of the model derived through a non-standard discretization of system (1.2) have been studied in [19]. Here, the approximation $x^2 \to x_n x_{n+1}$ has been adopted. The expression $x_n x_{n+1}$

assumes that the effect of individuals on their own population density is not instantaneous but also includes their influence at the next time step. In particular, interactions among individuals occur cumulatively and with delayed effects. In this study, we reexamine the model's qualitative behavior by applying an alternative non-standard finite difference discretization to the continuous predator-prey framework and employing a distinct bifurcation analysis technique. Originally developed by Mickens [34–36], this method has been used in a variety of biological systems. We adopted the approximation $xy \to x_{n+1}y_n$, which introduces forward localization for the prey variable in the predator-prey interaction term. This subtle but important difference allows our discretized model to better capture feedback mechanisms, such as delayed predation responses or inertia in ecological interactions, that are important in explaining real-life population dynamics. This choice is biologically motivated by the fact that the prey population can change more rapidly than the predator population over a single time step, particularly in systems with discrete generational structure. By using the updated prey value x_{n+1} instead of x_n, the model reflects the reality that predators interact with the most recently available prey population, thereby capturing the immediate ecological feedback more accurately. Furthermore, this formulation introduces a form of dynamic regulation: As the prey population increases, the predation pressure in the next iteration becomes stronger, naturally suppressing unchecked growth and preventing unrealistic population explosions. This enhanced feedback structure contributes to the preservation of key biological properties such as positivity and boundedness. Therefore, the approximation not only aligns with the principles of the NSFD scheme but also strengthens the ecological fidelity of the model by incorporating biologically realistic nonlinear dynamics.

For this purpose, we consider the analysis of a more advanced version of model (1.2):

$$\begin{aligned} x_{n+1} &= \frac{[kx_n + hrx_n(k - x_n)](1 + nx_n)}{k(1 + nx_n + h\alpha y_n)} \\ y_{n+1} &= y_n + h(\frac{\alpha\delta x_n y_n}{1 + nx_n} - y_n s) \end{aligned} \tag{1.3}$$

where h denotes the step size. x_n and y_n represent the prey and predator populations at generation n, respectively.

1.1. Comparison of positivity conditions in Euler and NSFD schemes

To ensure the biological viability of discrete-time predator-prey models, the positivity of the numerical solutions x_n and y_n must be guaranteed. Below, we compare the positivity conditions of two different discretization approaches—namely, the standard forward Euler method and the NSFD scheme.

1.1.1. Euler method discretization

The system discretized by the standard forward Euler method is given by:

$$\begin{aligned} x_{n+1} &= x_n + h\left[rx_n\left(1 - \frac{x_n}{k}\right) - \frac{\alpha x_n y_n}{1 + nx_n}\right], \\ y_{n+1} &= y_n + h\left[\frac{\alpha\delta x_n y_n}{1 + nx_n} - sy_n\right]. \end{aligned}$$

To ensure $x_{n+1} > 0$ and $y_{n+1} > 0$, we derive the following parameter-dependent bounds:

- **For x_n positivity:**

$$r\left(1 - \frac{x_n}{k}\right) > \frac{\alpha y_n}{1 + nx_n} - \frac{1}{h} \quad \Rightarrow \quad y_n < \frac{(nx_n + 1)(hkr - hrx_n + k)}{\alpha hk}.$$

- **For y_n positivity:**

$$1 + h\left(\frac{\alpha\delta x_n}{1 + nx_n} - s\right) > 0 \quad \Rightarrow \quad x_n > \frac{hs - 1}{\alpha\delta h - hns + n}.$$

These expressions indicate that the step size h, along with biological parameters such as r, α, δ, s, n, must be carefully chosen to maintain positive population values. Particularly, large h values may easily lead to numerical instability or biologically meaningless negative values.

1.1.2. NSFD scheme discretization

The corresponding system using the NSFD scheme is:

$$x_{n+1} = \frac{x_n(1 + nx_n)\,(hr(k - x_n) + k)}{k(1 + nx_n + h\alpha y_n)},$$
$$y_{n+1} = y_n \cdot \frac{h(\alpha\delta x_n - s(1 + nx_n)) + (1 + nx_n)}{1 + nx_n}.$$

- The expression for x_{n+1} is strictly positive for all $x_n > 0$, $y_n > 0$, and positive parameters, since it is composed of a product of positive terms divided by a positive denominator.
- For $y_{n+1} > 0$, the same condition as in the Euler case is obtained:

$$1 + h\left(\frac{\alpha\delta x_n}{1 + nx_n} - s\right) > 0 \quad \Rightarrow \quad x_n > \frac{hs - 1}{\alpha\delta h - hns + n}.$$

Generally, unlike the Euler method, the NSFD scheme incorporates parameter-driven nonlinear denominators that prevent blow-up and stabilize the system numerically, even for larger step sizes h.

1.1.3. Conclusion of comparison

While both schemes yield a similar analytical positivity condition for the predator population, the NSFD scheme offers superior structural preservation. Specifically:

- The NSFD model guarantees the positivity of the prey dynamics for all $x_n > 0$ and $y_n > 0$;
- Euler's method, by contrast, is highly sensitive to the step size h and may result in negative population values if not carefully tuned.

It also prevents numerical blow-up via its nonlinear denominator structure. Therefore, the NSFD scheme is more robust in preserving the qualitative dynamics of the original continuous-time model while maintaining biological realism. This supports the use of NSFD schemes in modeling population systems governed by nonlinear interactions and saturation effects.

In terms of stability, the forward Euler discretization of the predator-prey model reveals that local stability analysis around fixed points is sensitive to parameters and initial conditions. It is seen that the system exhibits multi-periodic behavior, and analysis with classical bifurcation theory is not possible [37]. In contrast, our framework not only ensures the positivity and boundedness of the solutions but also better captures the saturation effects encoded by Holling type II functional responses. As demonstrated analytically and numerically, the NSFD discretization more robustly preserves the stability nature of equilibria and reproduces bifurcation phenomena more closely to their theoretical values predicted by the continuum model. Specifically, while both methods detect bifurcation transitions, the Eulerian method tends to vary bifurcation thresholds and can lead to non-biological behaviors, such as varying population sizes, while the NSFD approach preserves the underlying dynamical structure. This structural consistency highlights the advantage of NSFD schemes in long-term ecological modeling and in the numerical simulation of discrete-time systems derived from biological dynamics. We therefore conclude that, compared to the Euler-based discretization, the NSFD framework provides a more accurate and biologically consistent approach for capturing the dynamical richness of predator-prey systems, particularly in the context of stability preservation and bifurcation characterization.

Moreover, while the forward Euler discretization approximates the dynamics of the continuous model, it does not guarantee fundamental biological properties such as positivity and boundedness under large step sizes or certain initial conditions. The NSFD scheme, on the other hand, modifies the denominator structure using saturating terms such as $1 + nx_n + h\alpha y_n$, which prevents uncontrolled growth when the population sizes increase. In particular, the model incorporates internal limiting mechanisms that become more effective when the predator population increases. Therefore, unlike the Euler method, the NSFD approach preserves boundedness and positivity, providing a more biologically realistic numerical structure without imposing artificial restrictions on the step size.

2. The existence and local stability of fixed points

This part focuses on determining the fixed points of the discrete predator-prey system (1.3) and analyzing their local stability. It can be observed that for any choice of the positive parameters r, α, δ, s, n and h, the system (1.3) possesses the trivial fixed point $\vartheta_1 = (0, 0)$ and the semi-trivial fixed point $\vartheta_2 = (k, 0)$. If $\alpha > \max\{\frac{ns}{\delta}, \frac{s(1+kn)}{\delta}\}$, then the system (1.3) has a positive fixed solution $\vartheta_3 = (\frac{s}{\alpha\delta - ns}, \frac{r\delta(k(\alpha\delta - ns) - s)}{k(\alpha\delta - ns)^2})$. The linearized form of system (1.3) at fixed solution $\vartheta = (x, y)$ under the map $(f, g) \to (x_{n+1}, y_{n+1})$ is characterized by its Jacobian matrix

$$J_{|_\vartheta} = \begin{pmatrix} a_{11} & a_{12} \\ a_{21} & a_{22} \end{pmatrix} \tag{2.1}$$

where

$$a_{11} = \frac{(1 + nx)^2(k + hkr - 2hrx) + h(k(1 + hr)(1 + 2nx) - hrx(2 + 3nx))y\alpha)}{k(1 + nx + hy\alpha)^2},$$

$$a_{12} = \frac{-h(1 + nx)(kx + hr(k - x)x)\alpha}{k(1 + nx + hy\alpha)^2}, a_{21} = \frac{hy\alpha\delta}{(1 + nx)^2}, a_{22} = 1 - hs + \frac{hx\alpha\delta}{1 + nx}$$

such that $f = \frac{[kx+hrx(k-x)](1+nx)}{k(1+nx+h\alpha y)}$ and $g = y+h(\frac{\alpha\delta xy}{1+nx}-ys)$. Based on current stability theory [38,39], we will now investigate the local dynamics of (1.3) at fixed solutions ϑ_i $(i = 1, 2, 3)$ by using the eigenvalues of the Jacobian matrix.

Theorem 1. *ϑ_1 of model (1.3) is never a sink. It is a source, a saddle and non-hyperbolic if $s > \frac{2}{h}$, $s < \frac{2}{h}$ and $s = \frac{2}{h}$, respectively.*

Proof. The $J_{|_{\vartheta_1}}$ evaluated at ϑ_1 is

$$J_{|_{\vartheta_1}} = \begin{pmatrix} 1+hr & 0 \\ 0 & 1-hs \end{pmatrix} \tag{2.2}$$

with $\lambda_1 = 1 + hr$ and $\lambda_2 = 1 - hs$. Since the h and s are positive parameters, $|\lambda_1| = 1 + hr > 1$, and so ϑ_1 is never sink. □

Theorem 2. *ϑ_2 of model (1.3) is (i) a sink if $r < \frac{2}{h}$ and $\frac{hs-2}{ha\delta-hsn+2n} < k < \frac{s}{a\delta-sn}$ (ii) a saddle if (ii.1) $r > \frac{2}{h}$ and $\frac{hs-2}{ha\delta-hsn+2n} < k < \frac{s}{a\delta-sn}$ or (ii.2) $r < \frac{2}{h}$ and $(k > \frac{s}{a\delta-sn}$ or $k < \frac{hs-2}{ha\delta-hsn+2n})$ (iii) a source if $r > \frac{2}{h}$ and $(k > \frac{s}{a\delta-sn}$ or $k < \frac{hs-2}{ha\delta-hsn+2n})$ (iv) non–hyperbolic if $r = \frac{2}{h}$ or $(k = \frac{s}{a\delta-sn}$ or $k = \frac{hs-2}{ha\delta-hsn+2n})$, where $hs > 2$, $a\delta > sn$.*

Proof. The $J_{|_{\vartheta_2}}$ evaluated at ϑ_2 is

$$J_{|_{\vartheta_2}} = \begin{pmatrix} 1-hr & -\frac{hk\alpha}{1+kn} \\ 0 & 1-hs+\frac{hk\alpha\delta}{1+kn} \end{pmatrix} \tag{2.3}$$

with $\lambda_1 = 1 - hr$ and $\lambda_2 = 1 - hs + \frac{hk\alpha\delta}{1+kn}$. Results can be easily achieved by calculations made on the eigenvalues. □

Theorem 3. *If $\Delta < 0$, then ϑ_3 is (i) a stable point if $\frac{hrs}{(1+hr)(\alpha\delta-ns)} < k < \frac{(\alpha\delta+s(n-hns+h\alpha\delta))}{(ns-\alpha\delta)(n(-1+hs)-h\alpha\delta)}$. (ii) an unstable point if $\frac{(\alpha\delta+s(n-hns+h\alpha\delta))}{(ns-\alpha\delta)(n(-1+hs)-h\alpha\delta)} < k < \frac{hrs}{(1+hr)(\alpha\delta-ns)}$. (iii) non-hyperbolic if $k = \frac{(\alpha\delta+s(n-hns+h\alpha\delta))}{(ns-\alpha\delta)(n(-1+hs)-h\alpha\delta)}$ or $k = \frac{hrs}{(1+hr)(ns-\alpha\delta)}$*
for $ns < \alpha\delta$.

Proof. By considering model (1.3), for ϑ_3, we obtain

$$J_{|_{\vartheta_3}} = \begin{pmatrix} (k\alpha\delta(-ns+\alpha\delta) & \\ -\frac{-hr(ns^2+kn^2s^2+\alpha\delta(2s-k\alpha\delta)))}{\alpha\delta(hrs+k(1+hr)(ns-\alpha\delta))} & -\frac{hks(ns-\alpha\delta)}{\delta(hrs+k(1+hr)(ns-\alpha\delta))} \\ -\frac{hr(s+kns-k\alpha\delta)}{k\alpha} & 1 \end{pmatrix} \tag{2.4}$$

with characteristic equation

$$\lambda^2 - \tilde{A}\lambda + \tilde{N} = 0 \tag{2.5}$$

where

$$\tilde{A} = \frac{(2k\alpha\delta(ns-\alpha\delta)+hr(kn^2s^2+\alpha\delta(3s-2k\alpha\delta)+ns(s+k\alpha\delta)))}{\alpha\delta(hrs+k(1+hr)(ns-\alpha\delta))}, \tag{2.6}$$

$$\tilde{N} = \frac{\begin{array}{c} k\alpha\delta(ns-\alpha\delta) + h^2rs(-ns+\alpha\delta)(s+kns-k\alpha\delta) \\ +hr(ns^2+kn^2s^2+\alpha\delta(2s-k\alpha\delta)) \end{array}}{\alpha\delta(hrs+k(1+hr)(ns-\alpha\delta))}. \tag{2.7}$$

So, we obtain the roots of the characteristic equation as

$$\lambda_{1,2} = \frac{\tilde{A} \mp \sqrt{\Delta}}{2} \tag{2.8}$$

where

$$\begin{aligned} \Delta &= \tilde{A}^2 - 4\tilde{N} \qquad (2.9)\\ &= \left(\frac{2k\alpha\delta(ns-\alpha\delta) + hr(kn^2s^2+\alpha\delta(3s-2k\alpha\delta)+ns(s+k\alpha\delta))}{\alpha\delta(hrs+k(1+hr)(ns-\alpha\delta))}\right)^2 - \\ &4\left(\frac{\begin{array}{c} k\alpha\delta(ns-\alpha\delta) + h^2rs(-ns+\alpha\delta)(s+kns-k\alpha\delta) \\ +hr(ns^2+kn^2s^2+\alpha\delta(2s-k\alpha\delta)) \end{array}}{\alpha\delta(hrs+k(1+hr)(ns-\alpha\delta))}\right). \end{aligned}$$

If $\Delta < 0$, then the roots are

$$\lambda_{1,2} = \frac{(2k\alpha\delta(ns-\alpha\delta) + hr(kn^2s^2+\alpha\delta(3s-2k\alpha\delta)+ns(s+k\alpha\delta)))}{2\alpha\delta(hrs+k(1+hr)(ns-\alpha\delta))} \mp \tag{2.10}$$
$$\frac{i}{2}\sqrt{\begin{array}{c} 4\left(\frac{k\alpha\delta(ns-\alpha\delta)+h^2rs(-ns+\alpha\delta)(s+kns-k\alpha\delta)+hr(ns^2+kn^2s^2+\alpha\delta(2s-k\alpha\delta))}{\alpha\delta(hrs+k(1+hr)(ns-\alpha\delta))}\right) - \\ \left(\frac{2k\alpha\delta(ns-\alpha\delta)+hr(kn^2s^2+\alpha\delta(3s-2k\alpha\delta)+ns(s+k\alpha\delta))}{\alpha\delta(hrs+k(1+hr)(ns-\alpha\delta))}\right)^2 \end{array}}$$

and if $\left|\lambda_{1,2}\right| = \sqrt{\frac{(hn(1+kn)rs^2(1-hs)+s(kn+2hr+h^2(1+2kn)rs)\alpha\delta-k(1+hr(1+hs))\alpha^2\delta^2)}{\alpha\delta(hrs+k(1+hr)(ns-\alpha\delta))}} < 1$, equivalently, $\frac{hrs}{(1+hr)(\alpha\delta-ns)} < k < \frac{\alpha\delta+s(n-hns+h\alpha\delta)}{(ns-\alpha\delta)(n(-1+hs)-h\alpha\delta)}$, $ns < \alpha\delta$, then ϑ_3 is a stable point. Also, one can find that ϑ_3 is an unstable point if $\frac{\alpha\delta+s(n-hns+h\alpha\delta)}{(ns-\alpha\delta)(n(-1+hs)-h\alpha\delta)} < k < \frac{hrs}{(1+hr)(\alpha\delta-ns)}$ and ϑ_3 is a non-hyperbolic point if $k = \frac{\alpha\delta+s(n-hns+h\alpha\delta)}{(ns-\alpha\delta)(n(-1+hs)-h\alpha\delta)}$ or $k = \frac{hrs}{(1+hr)(\alpha\delta-ns)}$. □

3. Bifurcation analysis

In this part, we first examine the bifurcation analysis of discrete system (1.3) using bifurcation theory [40]. For the considered model (1.3), a flip bifurcation may occur at ϑ_1 if $(r, \alpha, \delta, s, n, h, k)$ passes throughout the region:

$$\Theta\,|_{\vartheta_1} = \left\{(r, \alpha, \delta, s, n, h, k),\ s = \frac{2}{h}\right\} \tag{3.1}$$

where ϑ_1 is non-hyperbolic point when $s = \frac{2}{h}$. Then one has $\lambda_2\,|_{s=\frac{2}{h}} = -1$, and $\lambda_1\,|_{s=\frac{2}{h}} = 1+hr \neq 1$ or -1. However, according to calculation, a flip bifurcation does not occur at ϑ_1 if $(r, \alpha, \delta, s, n, h, k) \in \Theta\,|_{\vartheta_1}$.

Based on the result that ϑ_2 is a non-hyperbolic if $k = \frac{hs-2}{2n-hsn+h\alpha\delta}$, one gets $\lambda_2\,|_{k=\frac{hs-2}{2n-hsn+h\alpha\delta}} = -1$ and $\lambda_1\,|_{k=\frac{hs-2}{2n-hsn+h\alpha\delta}} = 1-hr \neq 1$. It can be verified through straightforward calculation that system (1.3)

exhibits a flip bifurcation at ϑ_2 when $k = \frac{hs-2}{2n-hsn+h\alpha\delta}$. Moreover, the system (1.3) does not exhibit a flip bifurcation when $r = \frac{2}{h}$, since non-degeneracy conditions are not met.

Now let's examine the change in the dynamics of system (1.3) at ϑ_3. If the value $k = \frac{\alpha\delta+s(n-hns+h\alpha\delta)}{(ns-\alpha\delta)(n(-1+hs)-h\alpha\delta)}$ is considered, then $\left|\lambda_{1,2}\right| \mid_{k=\frac{\alpha\delta+s(n-hns+h\alpha\delta)}{(ns-\alpha\delta)(n(-1+hs)-h\alpha\delta)}} = 1$ holds for the pair of complex characteristic roots of the Jacobian matrix J at ϑ_3. As a result, model (1.3) may experience Neimark–Sacker bifurcation at ϑ_3 if $(r, \alpha, \delta, s, n, h, k)$ passes through the pointed out curve below:

$$\Omega \mid_{\vartheta_3} = \left\{(r, \alpha, \delta, s, n, h, k),\ k = \frac{\alpha\delta + s(n - hns + h\alpha\delta)}{(ns - \alpha\delta)(n(-1 + hs) - h\alpha\delta)}, \Delta < 0\right\}. \tag{3.2}$$

For $k \in \Omega \mid_{\vartheta_3}$, we get

$$\frac{\partial \left|\lambda_i(k)\right|}{\partial k} \mid_{k=\frac{\alpha\delta+s(n-hns+h\alpha\delta)}{(ns-\alpha\delta)(n(-1+hs)-h\alpha\delta)}} \neq 0\ ,\ i = 1, 2, \tag{3.3}$$

and if

$$\frac{hn(1 + kn)rs^2 + (3hr + kn(2 + hr))s\alpha\delta - 2k(1 + hr)\alpha^2\delta^2}{(\alpha\delta(-hrs + k(1 + hr)(\alpha\delta - ns)))}|_k \neq 0, -1, \tag{3.4}$$

then

$$\lambda^m(k) \neq 1 \text{ for } m = 1, 2, 3, 4, \tag{3.5}$$

is satisfied.

By considering (3.2) and (2.4), we have

$$\widehat{A} = \begin{pmatrix} \frac{-ns(1-hs+h^2rs)+(-1+h^2rs-h(r+s))\alpha\delta)}{(ns(-1+hs)-(1+h(r+s))\alpha\delta)} & \frac{(hs(ns(-1+hs)-(1+hs)\alpha\delta))}{(\delta(n(s-hs^2)+(1+h(r+s))\alpha\delta))} \\ \frac{(hr\delta(-ns+\alpha\delta))}{(n(s-hs^2)+(1+hs)\alpha\delta)} & 1 \end{pmatrix}. \tag{3.6}$$

Let q and p be the eigenvectors of the matrices $\widehat{A}$ and $\widehat{A}^T$ corresponding to λ and $\overline{\lambda}$, respectively. For direct calculation, we use

$$\begin{aligned} \widehat{A}\, q = \lambda q,\ \widehat{A}\, \overline{q} = \lambda \overline{q}, \\ \widehat{A}^T p = \overline{\lambda} p,\ \widehat{A}^T \overline{p} = \overline{\lambda}\overline{p}. \end{aligned} \tag{3.7}$$

If p is normalized with respect to q, then it is clear that $< p, q >= 1$ for the resulting vector p, with the scalar product in $\mathbb{C}^2$ given by $< p, q >= \overline{p_1}q_1 + \overline{p_2}q_2$. Using the transformation $u = x - \frac{s}{\alpha\delta-ns}$, $v = y - \frac{r\delta(k(\alpha\delta-ns)-s)}{k(\alpha\delta-ns)^2}$, the fixed point ϑ_3 is shifted to the origin. So, we obtain

$$\begin{pmatrix} u \\ v \end{pmatrix} \to J_{\vartheta_3}\begin{pmatrix} u \\ v \end{pmatrix} + \begin{pmatrix} F_1(u, v) \\ F_2(u, v) \end{pmatrix} \tag{3.8}$$

where

$$\begin{aligned} F_1(u, v) = \frac{hr(ns - \alpha\delta)}{\alpha^2\delta^2\left(hrs + k(1 + hr)(ns - \alpha\delta)\right)^2} \cdot \Big[& - hrs\alpha\delta(2ns + \alpha\delta) \\ & + k^2 n(ns - \alpha\delta)^2\left(ns - (1 + hr)\alpha\delta\right) \end{aligned}$$

$$
\begin{aligned}
&+ k(ns-\alpha\delta)\left(n^2s^2 - n(1+3hr)s\alpha\delta - (1+hr)\alpha^2\delta^2\right)\Big]u^2 \\
&+ \frac{hk(ns-\alpha\delta)^2}{\alpha\delta^2\left(hrs + k(1+hr)(ns-\alpha\delta)\right)^2}\cdot\Big[hrs(ns+2\alpha\delta) \\
&+ k(ns-\alpha\delta)\left(n(-1+hr)s + (1+hr)\alpha\delta\right)\Big]uv \\
&- \frac{h^2k^2s(ns-\alpha\delta)^3}{\delta^2\left(hrs + k(1+hr)(ns-\alpha\delta)\right)^2}v^2 \\
&+ \frac{hnr(ns-\alpha\delta)^2(s+kns-k\alpha\delta)}{\alpha^3\delta^3\left(hrs + k(1+hr)(ns-\alpha\delta)\right)^3}\cdot\Big[hr\alpha\delta + kn(-ns+\alpha\delta)\Big]\cdot \\
&\Big[hrs\alpha\delta - k(ns-\alpha\delta)\left(ns-(1+hr)\alpha\delta\right)\Big]u^3 + O(\|U\|^4)
\end{aligned} \tag{3.9}
$$

$$
\begin{aligned}
F_2(u,v) = \frac{-hnr(ns-\alpha\delta)(s+kns-k\alpha\delta)}{k\alpha^2\delta}u^2 + \frac{h(ns-\alpha\delta)^2}{\alpha\delta}uv \\
\frac{-hn^2r(ns-\alpha\delta)^2(s+kns-k\alpha\delta)}{k\alpha^3\delta^2}u^3 + \mathrm{O}(\|U\|^4)
\end{aligned} \tag{3.10}
$$

such that $U_n = (u_n, v_n)^T$. Accordingly, system (3.8) can be reformulated as follows:

$$
(U_{n+1}) \to J_{\vartheta_3}(U_n) + \frac{1}{2}B(u_n,u_n) + \frac{1}{6}C(u_n,u_n,u_n) + O(\|U_n\|^4), \tag{3.11}
$$

with the multilinear vector functions of $u, v, w \in \mathbb{R}^2$:

$$
B(u,v) = \begin{pmatrix} B_1(u,v) \\ B_2(u,v) \end{pmatrix} \tag{3.12}
$$

and

$$
C(u,v,w) = \begin{pmatrix} C_1(u,v,w) \\ C_2(u,v,w) \end{pmatrix}. \tag{3.13}
$$

The following forms define these vectors

$$
\begin{aligned}
B_1(u,v) = \sum_{j,k=1}^{2} \frac{\partial^2 F_1}{\partial\xi_j\partial\xi_k}\,|_{\xi=0}\; u_jv_k = \\
\frac{\begin{array}{c}2hr(ns-\alpha\delta)(-hrs\alpha\delta(2ns+\alpha\delta) + k^2n(ns-\alpha\delta)^2(ns-(1+hr)\alpha\delta) \\ +k(ns-\alpha\delta)(n^2s^2 - n(1+3hr)s\alpha\delta - (1+hr)\alpha^2\delta^2))\end{array}}{\alpha^2\delta^2(hrs + k(1+hr)(ns\text{-}\alpha\delta))^2}u_1v_1 \\
\frac{\begin{array}{c}hk(ns-\alpha\delta)^2(hrs(ns+2\alpha\delta) + k(ns-\alpha\delta) \\ (n(-1+hr)s + (1+hr)\alpha\delta))\end{array}}{\alpha\delta^2(hrs + k(1+hr)(ns-\alpha\delta))^2}(u_2v_1 + u_1v_2) \\
-\frac{2h^2k^2s(ns-\alpha\delta)^3}{\delta^2(hrs + k(1+hr)(ns-\alpha\delta))^2}u_2v_2,
\end{aligned} \tag{3.14}
$$

$$B_2(u,v) = \sum_{j,k=1}^{2} \frac{\partial^2 F_2}{\partial \xi_j \partial \xi_k} \mid_{\xi=0} u_j v_k = \frac{-2hnr(ns-\alpha\delta)(s+kns-k\alpha\delta)}{k\alpha^2\delta} u_1 v_1 + \frac{h(ns-\alpha\delta)^2}{\alpha\delta(u_2 v_1 + u_1 v_2)}(u_2 v_1 + u_1 v_2)$$

and

$$C_1(u,v,w) = \sum_{j,k=1}^{2} \frac{\partial^3 F_1}{\partial \xi_j \partial \xi_k \xi_l} \mid_{\xi=0} u_j v_k w_l = \frac{6hnr(ns-\alpha\delta)^2(s+kns-k\alpha\delta)(hr\alpha\delta+kn(-ns+\alpha\delta))(hrs\alpha\delta-k(ns-\alpha\delta)(ns-(1+hr)\alpha\delta))}{\alpha^3\delta^3(hrs+k(1+hr)(ns-\alpha\delta))^3} u_1 v_1 w_1, \tag{3.15}$$

$$C_2(u,v,w) = \sum_{j,k=1}^{2} \frac{\partial^3 F_2}{\partial \xi_j \partial \xi_k \xi_l} \mid_{\xi=0} u_j v_k w_l = \frac{-6hn^2 r(ns-\alpha\delta)^2(s+kns-k\alpha\delta)}{k\alpha^3\delta^2} u_1 v_1 w_1$$

and $k = \frac{\alpha\delta+s(n-hns+h\alpha\delta)}{(ns-\alpha\delta)(n(-1+hs)-h\alpha\delta)}$.

$\forall\ U \in \mathbb{R}^2$ can be expressed uniquely in the form

$$U = zq + \overline{zq}$$

where $z \in \mathbb{C}$, and $\overline{z}$ is the complex conjugate of z. Additionally $z =< p, U >$. For sufficiently small $|k|$ around k, we can transform the system (1.3) as follows:

$$z \to \lambda(k)z + g(z,\overline{z},k). \tag{3.16}$$

Here, $\lambda(k) = (1+\omega(k))e^{i\theta(k)}$ with $\omega(k) = 0$. The function $g(z,\overline{z},k)$ is a complex-valued smooth function of z and $\overline{z}$. The Taylor expansion of g with respect to z and $\overline{z}$ is

$$g(z,\overline{z},k) = \sum_{v+l\geq 2} \frac{1}{v!l!} g_{vl}(k) z^v \overline{z}^l$$

where g_{vl} are the Taylor coefficients, calculated using multilinear vector functions:

$$\begin{aligned} g_{20}(k) &=< p, B(q,q) > \\ g_{11}(k) &=< p, B(q,\overline{q}) > \\ g_{02}(k) &=< p, B(\overline{q},\overline{q}) > \\ g_{21}(k) &=< p, C(q,q,\overline{q}) > . \end{aligned} \tag{3.17}$$

For the system (3.8) undergoing Neimark–Sacker bifurcation, the direction of invariant curve emergence is governed by the coefficient $\varphi(k)$, which may be computed as

$$\varphi(k) = Re(\frac{e^{-i\theta(k)}g_{21}}{2}) - Re\left(\frac{(1-2e^{i\theta(k)})e^{-2i\theta(k)}}{2(1-e^{i\theta(k)})} g_{20}g_{11}\right) \tag{3.18}$$

$$-\frac{1}{2}|g_{11}|^2-\frac{1}{4}|g_{02}|^2$$

where $e^{i\theta(k)}=\lambda(k)$. Since $\varphi(k)\neq 0$, we establish through the following theorem that model (1.3) exhibits a Neimark–Sacker bifurcation at ϑ_3.

Theorem 4. *At ϑ_3, model (1.3) experiences a Neimark–Sacker bifurcation by taking $k=\frac{\alpha\delta+s(n-hns+h\alpha\delta)}{(ns-\alpha\delta)(n(-1+hs)-h\alpha\delta)}$ as a bifurcation parameter if $(r,\alpha,\delta,s,n,h,k)\in\Omega\,|_{\vartheta_3}$.*

Remark 1. *Provided that condition (3.4) holds, $\varphi(k)\neq 0$, and the parameter k lies within a sufficiently small neighborhood of $\Omega\,|_{\vartheta_3}$, the system (1.3) undergoes a Neimark–Sacker bifurcation at the unique fixed point ϑ_3. Moreover if $\varphi(k)<0$ a unique attracting invariant closed curve bifurcates from ϑ_3, whereas $\varphi(k)>0$, the bifurcating invariant closed curve is repelling.*

4. Chaos control

Chaos control theory provides a way to better understand mathematical models that exhibit chaotic behavior. Chaos control techniques applied within this theory aim to stabilize chaotic behavior that jumps from one periodic orbit to another in an irregular manner with the help of a specific control variable. Controlling chaos is based on the idea that intelligent selection of this perturbation can direct the trajectory to the desired location and produce a series of desired dynamic states. There are various techniques for chaos control. The OGY method developed by E. Ott, C. Grebogi, and J. A. Yorke [41] is one of the first fundamental observations of chaos control strategies. Usually, only very small perturbations are applied to an infinite number of unstable periodic orbits embedded in a chaotic attractor so that there is no significant change in the natural dynamics of the system. Thus, through small system perturbations, one or more of the unstable periodic orbits are stabilized, and a chaotic motion becomes more stable and predictable [42,43]. The state feedback method is another frequently used control strategy [38,44]. Although the OGY method is known to be ineffective for discrete-time models derived from continuous systems using the standard Euler discretization due to its inability to preserve key dynamical properties such as positivity and boundedness [45,46], this limitation does not apply in the present study. Here, the system is formulated using an NSFD scheme, which ensures the preservation of essential qualitative features of the original continuous model, including fixed point structure and stability properties. The NSFD approach yields a more faithful discrete analogue of the ecological dynamics, thereby enabling the successful implementation of the OGY control strategy. This modeling framework mitigates the shortcomings observed in Euler–discretized systems, such as artificial destabilization or deviation from biological realism, and provides a more robust platform for chaos control applications.

In our study, the underlying system is a discrete-time predator-prey model formulated with the NSFD scheme. This structure allows for biologically realistic dynamics while also enabling the implementation of control strategies to mitigate chaotic oscillations. From an ecological perspective, the application of control methods such as the OGY method and state feedback control can be interpreted as external interventions that stabilize the system around desired equilibrium or periodic states. These controls become particularly important in scenarios where the ecosystem experiences a loss of equilibrium due to environmental shocks, overexploitation, or delayed responses between predator and prey populations. In our discrete model, the OGY method is implemented by slightly

perturbing a parameter (e.g., intrinsic prey growth rate, prey-to-predator conversion efficiency, or predation pressure) when the system's state enters a small neighborhood of an unstable periodic orbit. This is biologically analogous to adjusting resource input, nutrient supplementation, or predator migration rates in response to observed population fluctuations; these interventions are reasonable in controlled ecosystems such as fisheries, predation, reserves or agricultural pest management. State feedback control, on the other hand, is implemented by designing a corrective force proportional to the deviation of population densities from desired values. This can be interpreted as adaptive harvesting, stocking, habitat restructuring, or predation pressure, where managers dynamically intervene in response to population data. For example, in predator management, targeted removal or conservation efforts based on real-time prey levels could reflect such feedback logic. Here, in addition to the state feedback control strategy, we will also use the OGY method for our nonstandard discretization model.

To apply the OGY approach, δ is taken as a control parameter. δ is restricted within the small interval $|\delta - \delta_0| < \overline{\nu}$ where $\overline{\nu} > 0$, with δ_0 denoting the nominal value in the chaotic domain. We examine $(\overline{x}, \overline{y})$, an unstable fixed point of system (1.3) emerging from Neimark–Sacker bifurcation in this chaotic region. The system (1.3) can be rewritten as indicated below in order to use the OGY technique:

$$\begin{bmatrix} x_{n+1} - \overline{x} \\ y_{n+1} - \overline{y} \end{bmatrix} \approx A \begin{bmatrix} x_n - \overline{x} \\ y_n - \overline{y} \end{bmatrix} + B[\delta - \delta_0] \tag{4.1}$$

where

$$\begin{aligned} A &= \begin{bmatrix} \frac{\partial f(\overline{x},\overline{y},\delta_0)}{\partial x_n} & \frac{\partial f(\overline{x},\overline{y},\delta_0)}{\partial y_n} \\ \frac{\partial g(\overline{x},\overline{y},\delta_0)}{\partial x_n} & \frac{\partial g(\overline{x},\overline{y},\delta_0)}{\partial y_n} \end{bmatrix} \\ &= \begin{bmatrix} -\frac{k\alpha\delta_0(-ns+\alpha\delta_0)-hr(ns^2+kn^2s^2+\alpha\delta_0(2s-k\alpha\delta_0))}{\alpha\delta_0(hrs+k(1+hr)(ns-\alpha\delta_0))} & -\frac{hks(ns-\alpha\delta_0)}{\delta_0(hrs+k(1+hr)(ns-\alpha\delta_0))} \\ -\frac{hr(s+kns-k\alpha\delta_0)}{k\alpha} & 1 \end{bmatrix} \end{aligned}$$

and

$$B = \begin{bmatrix} \frac{\partial f(\overline{x},\overline{y},\delta_0)}{\partial \delta} \\ \frac{\partial g(\overline{x},\overline{y},\delta_0)}{\partial \delta} \end{bmatrix} = \begin{bmatrix} 0 \\ -\frac{hrs(s+kns-k\alpha\delta_0)}{k(ns-\alpha\delta_0)^2} \end{bmatrix}.$$

The stabilization of system (1.3) is achieved through the control matrix:

$$C = [B : AB] = \begin{bmatrix} 0 & \frac{h^2rs^2(ns-\alpha\delta_0)(s+kns-k\alpha\delta_0)}{\delta(hrs+k(1+hr)(ns-\alpha\delta_0))(ns-\alpha\delta_0)^2} \\ -\frac{hrs(s+kns-k\alpha\delta_0)}{k(ns-\alpha\delta_0)^2} & -\frac{hrs(s+kns-k\alpha\delta_0)}{k(ns-\alpha\delta_0)^2} \end{bmatrix} \tag{4.2}$$

such that the rank of C is 2.

Moreover, we suppose that $[\delta - \delta_0] = -K \begin{bmatrix} x_n - \overline{x} \\ y_n - \overline{y} \end{bmatrix}$, where $K = \begin{bmatrix} \rho_1 & \rho_2 \end{bmatrix}$, then the system (4.1) can be written as

$$\begin{bmatrix} x_{n+1} - \overline{x} \\ y_{n+1} - \overline{y} \end{bmatrix} \approx [A - BK] \begin{bmatrix} x_n - \overline{x} \\ y_n - \overline{y} \end{bmatrix}. \tag{4.3}$$

The controlled system can be mathematically represented as

$$x_{n+1} = \frac{[kx_n + hrx_n(k - x_n)](1 + nx_n)}{k(1 + nx_n + h\alpha y_n)}$$
$$y_{n+1} = y_n + h(\frac{\alpha[\delta_0 - \rho_1(x_n - \overline{x}) - \rho_2(y_n - \overline{y})]x_n y_n}{1 + nx_n} - y_n s). \tag{4.4}$$

The fixed point $(\overline{x}, \overline{y})$ becomes locally asymptotically stable if and only if the characteristic roots μ_1 and μ_2 of the $A - BK$ satisfy the stability criterion $|\mu_i| < 1$. This control matrix for system (4.4) is determined to be:

$$A - BK = \begin{bmatrix} M_{11} & M_{12} \\ M_{21} & M_{22} \end{bmatrix}, \tag{4.5}$$

where

$$M_{11} = \frac{-hn(1 + kn)rs^2 - (kn + 2hr)s\alpha\delta_0 + k(1 + hr)\alpha^2\delta_0^2}{\alpha\delta_0\left[-(hr + k(n + hnr))s + k(1 + hr)\alpha\delta_0\right]},$$
$$M_{12} = \frac{hks(ns - \alpha\delta_0)}{\delta_0\left[-(hr + k(n + hnr))s + k(1 + hr)\alpha\delta_0\right]},$$
$$M_{21} = \frac{-hr(s + kns - k\alpha\delta_0)\left[(ns - \alpha\delta_0)^2 - s\alpha\rho_1\right]}{k\alpha(ns - \alpha\delta_0)^2},$$
$$M_{22} = 1 + \frac{hrs(s + kns - k\alpha\delta_0)\rho_2}{k(ns - \alpha\delta_0)^2}.$$

The characteristic equation associated with the Jacobian matrix $A - BK$ is given by

$$\mu^2 - (M_{11} + M_{22})\mu + P = 0,$$

where $P = M_{11}M_{22} - M_{12}M_{21}$ is the determinant of the Jacobian matrix.

Let μ_1 and μ_2 solve the characteristic equation of system (4.4). Then the following relationship holds

$$\mu_1 + \mu_2 = M_{11} + M_{22}, \tag{4.6}$$

$$\mu_1\mu_2 = P. \tag{4.7}$$

Stability boundaries are determined by $\mu_1 = \pm 1$ and $\mu_1\mu_2 = 1$. If $\mu_1\mu_2 = 1$, then from Eq (4.7), we get

$$l_1 = P - 1 = 0. \tag{4.8}$$

Substituting $\mu_1 = 1$, into the Eqs (4.6) and (4.7), we reach

$$l_2 := M_{11} + M_{22} - P - 1 = 0. \tag{4.9}$$

Analogously, for the case $\mu_1 = -1$, applying Eqs (4.6) and (4.7) yields

$$l_3 := M_{11} + M_{22} + P + 1 = 0. \tag{4.10}$$

The triangular domain bounded by the lines l_1, l_2, and l_3 in the $\rho_1\rho_2$-plane constitutes the parameter region where all eigenvalues satisfy $|\mu_i| < 1$.

We will now investigate chaotic control using the state feedback control approach. To do this, in the model (1.3), one can add control force $F_n = -\tau_1(x_n - \overline{x}) - \tau_2(y_n - \overline{y})$ with gain coefficients $\tau_{1,2}$

$$\begin{aligned} x_{n+1} &= \frac{[kx_n + hrx_n(k - x_n)](1 + nx_n)}{k(1 + nx_n + h\alpha y_n)} + F_n \\ y_{n+1} &= y_n + h(\frac{\alpha x_n y_n}{1 + nx_n} - y_n s) \end{aligned} \tag{4.11}$$

where $(\overline{x}, \overline{y}) = (\frac{s}{\alpha\delta - ns}, \frac{r\delta(k(\alpha\delta - ns) - s)}{k(\alpha\delta - ns)^2})$. The Jacobian matrix $J(\overline{x}, \overline{y})$ takes the form

$$\begin{bmatrix} -\dfrac{A_1\tau_1}{A_2} & -\dfrac{hks\gamma(ns - \alpha\delta)}{\delta A_2} - \tau_2 \\ -\dfrac{hr\gamma(s + kns - k\alpha\delta)}{k\alpha} & 1 \end{bmatrix},$$

where

$$\begin{aligned} A_1 &= hn(1 + kn)rs^2 + (kn + 2hr)s\alpha\delta - k(1 + hr)\alpha^2\delta^2 \\ &\quad - \alpha\delta(hrs + k(1 + hr)(ns - \alpha\delta)), \\ A_2 &= \alpha\delta(hrs + k(1 + hr)(ns - \alpha\delta)), \end{aligned}$$

and the characteristic equation is

$$\eta^2 - \frac{A_1}{A_2}\eta - \frac{kA_1(-k\alpha\tau_1 - hr(s + kns - k\alpha\delta)\tau_2)}{k\alpha A_2} = 0. \tag{4.12}$$

The roots of this quadratic equation, η_1 and η_2, determine the local stability and bifurcation properties near the fixed point.

Considering these characteristic roots η_1 and η_2, we obtain the fundamental relation

$$\eta_1 + \eta_2 = \frac{A_1}{A_2}, \tag{4.13}$$

$$\eta_1\eta_2 = -\frac{kA_1(-k\alpha\tau_1 - hr(s + kns - k\alpha\delta)\tau_2)}{k\alpha A_2}. \tag{4.14}$$

Marginal stability requires $\eta_1 = \pm 1$ and $\eta_1\eta_2 = 1$. To determine the marginal stability boundaries of a discrete-time dynamical system, one typically analyzes the characteristic equation derived from the system's linearization around an equilibrium point. The critical thresholds where stability changes occur correspond to specific values of the characteristic roots—in particular, when the eigenvalues (denoted μ_1 and μ_2) lie on the unit circle in the complex plane. The condition $\mu_1\mu_2 = 1$ corresponds to the boundary where the determinant of the linearized system equals one, which is typically used to detect Neimark–Sacker bifurcations. In contrast, $\mu_1 = -1$ and $\mu_1 = +1$ indicate the occurrence of flip (period-doubling) and fold (saddle-node) bifurcations, respectively. Let us take $\eta_1\eta_2 = 1$. Then from Eq (4.14), we obtain

$$L_1 := \frac{kA_1(-k\alpha\tau_1 - hr(s + kns - k\alpha\delta)\tau_2)}{k\alpha A_2} + 1 = 0. \tag{4.15}$$

By examining the case $\eta_1 = 1$ and simultaneously considering Eqs (4.13) and (4.14), we find that

$$L_2 := \frac{A_1}{A_2} - 1 + \frac{A_1(k\alpha\tau_1 + hr(s + kns - k\alpha\delta)\tau_2)}{\alpha A_2} = 0. \tag{4.16}$$

If $\eta_1 = -1$, by using Eqs (4.13) and (4.14), we obtain

$$L_3 := -\left(\frac{A_1}{A_2} + 1\right) + \frac{A_1(k\alpha\tau_1 + hr(s + kns - k\alpha\delta)\tau_2)}{\alpha A_2} = 0. \tag{4.17}$$

The triangle formed by the lines L_1, L_2, and L_3 in the $\eta_1\eta_2$-plane defines the set of values for which the eigenvalues have magnitudes less than 1.

5. Numerical simulations

This section presents numerical simulations to illustrate the occurrence of Neimark–Sacker bifurcation in system (1.3). Theoretical results are supported by selected examples under specific parameter values. The simulations reveal complex dynamical behaviors, particularly around the positive coexistence fixed point ϑ_3. Bifurcation diagrams, phase portraits, time series graph, and the Maximum Lyapunov Exponent (MLE) are provided to illustrate the dynamic nature of the system (1.3). The MLE is a key indicator used to characterize the stability and sensitivity of a dynamical system to initial conditions. Mathematically, it quantifies the average exponential rate of divergence (or convergence) between two infinitesimally close trajectories in phase space. A positive MLE value indicates chaotic behavior, while a negative value implies asymptotic stability. In discrete-time systems, MLE is particularly useful for detecting transitions to chaos via bifurcations such as period-doubling or Neimark–Sacker. The computation of the MLE involves evaluating the Jacobian matrix along the trajectory and measuring the growth rate of perturbations over time. This allows one to rigorously assess whether the system exhibits chaotic dynamics under varying parameter regimes. Diagrams are provided to verify the theoretical results via SageMath programming [47] and the Mathematica software.

Example 1. *Let us consider the following population model, where the parameter values* $n = 0.88, h = 1.15, s = 0.16, \alpha = 0.95, \delta = 0.6, r = 0.85$ *are taken from [19]. Computation yields the positive fixed point* $\vartheta_3 = (0.372787, 0.857596)$. *According to the given values, the system (1.3) has the following form:*

$$\begin{aligned} x_{n+1} &= \frac{(1.33964x_n + 0.9775x_n(1.33964 - x_n))(1 + 0.88x_n)}{1.33964(1 + 0.88x_n + 1.0925y_n)}, \\ y_{n+1} &= y_n + 1.15(\frac{0.57x_ny_n}{1 + 0.88x_n} - 0.16y_n) \end{aligned} \tag{5.1}$$

where $k = 1.33964$ *and the initial conditions* $x_0 = 0.54$ *and* $y_0 = 0.85$. *From (3.6), we obtain*

$$\widehat{A}_\Lambda = \begin{pmatrix} 0.942688 & -0.179812 \\ 0.318732 & 1 \end{pmatrix}.$$

The eigenvalues are

$$\lambda_{1,2} = 0.971344 \pm 0.237678i$$

with $\left|\lambda_{1,2}\right| = 1$. *Let* $q, p \in \mathbb{C}^2$ *be two eigenvectors corresponding to the eigenvalues* $\lambda_{1,2}$, *respectively. The eigenvector solutions are obtained using the Mathematica software as follows:*

$$q \sim (-0.0718871 + 0.596244i, 0.799578)^T$$

and

$$p \sim (0.799578, 0.0718871 - 0.596244i)^T.$$

For $< p, q >= 1$, *we set*

$$p \sim (3.05135.10^{-17} + 0.838583i, 0.62533 + 0.0753939i).$$

From (3.9), (3.10), (3.14), *and* (3.15), *one can obtain*

$$\begin{aligned} F_1(u,v) &= -0.237156u^2 - 0.191356u^3 - 0.38484uv + 0.0867313v^2 \\ F_2(u,v) &= -0.2112u^2 + 0.139946u^3 + 0.371657uv, \end{aligned}$$

$$\begin{aligned} B_1(u,v) &= -0.474312u_1v_1 - 0.38484(u_2v_1 + u_1v_2) + 0.173463u_2v_2 \\ B_2(u,v) &= -0.422399u_1v_1 + 0.371657(u_2v_1 + u_1v_2), \end{aligned}$$

and

$$\begin{aligned} C_1(u,v,w) &= -1.14813u_1v_1w_1 \\ C_2(u,v,w) &= 0.839676u_1v_1w_1. \end{aligned}$$

By using the formula (3.17), *the coefficients* g_{vl} *are*

$$\begin{aligned} g_{20}(k) &= -0.178345 - 0.0331392i \\ g_{11}(k) &= -0.121985 + 0.0280679i \\ g_{02}(k) &= -0.399421 - 0.684511i \\ g_{21}(k) &= -0.207051 + 0.089595i. \end{aligned}$$

From (3.18), *we have* $\varphi(k) = -0.368689$.

Example 1 illustrates the emergence of quasiperiodic dynamics due to a Neimark–Sacker bifurcation under biologically meaningful parameter values. From an ecological standpoint, this indicates a transition from stable coexistence to oscillatory population behavior, which often reflects natural cycles such as predator-prey boom-and-bust regimes. The bifurcation diagram in Figure 1(a) shows that as the bifurcation parameter k increases beyond a critical threshold, the fixed point loses stability and an invariant closed curve emerges. This leads to sustained oscillations in both prey and predator densities, as observed in the phase portraits (Figure 1(b)–(d)). Such behavior can represent ecological systems where the predator-prey interaction is subject to internal delays or inertia, resulting in populations that do not settle to a fixed equilibrium but fluctuate in a regular manner. The accompanying MLE plot (Figure 1(e)) confirms this transition by showing a change from negative to near-zero values, implying a loss of asymptotic stability and the onset of quasiperiodicity. Biologically, these dynamics suggest that minor environmental or interaction-based changes (reflected by variation in k) can drastically alter the population behavior from stability to persistent oscillations. This reinforces the importance of considering nonlinear feedback and time-discrete effects in ecosystem modeling, particularly when designing strategies for species conservation or pest control.

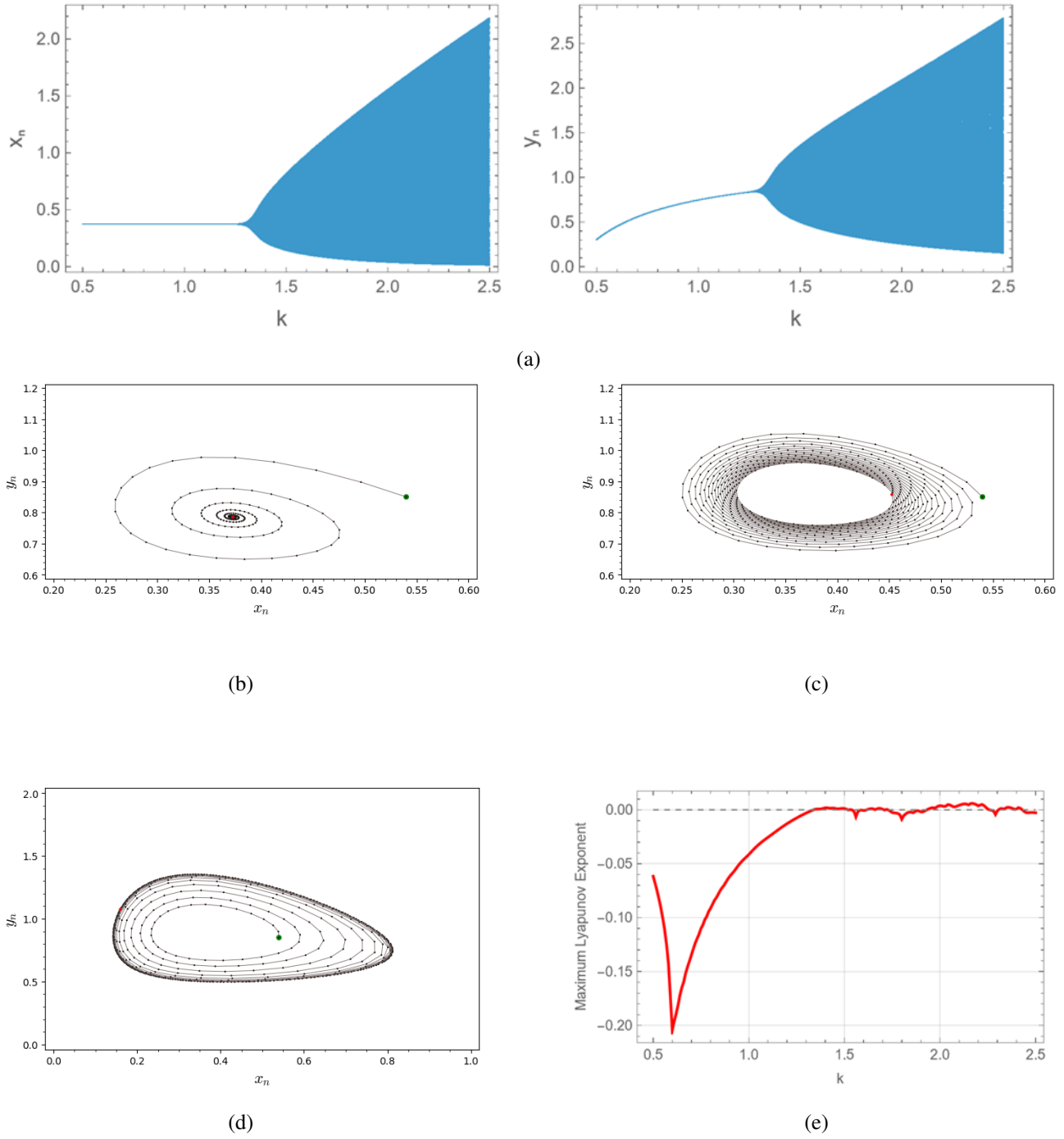

Figure 1. **(a)** *Neimark–Sacker bifurcation diagram of prey and predator densities in system (5.1) when* $n = 0.88, h = 1.15, s = 0.16, \alpha = 0.95, \delta = 0.6, r = 0.85$, *and* $k \in (0.5, 2.5)$. **(b)** *The phase portrait of system (5.1) when* $k = 1.1$. **(c)** *The phase portrait of system (5.1) when* $k = 1.33964$. **(d)** *The phase portrait of system (5.1) when* $k = 1.5$. **(e)** *Maximum Lyapunov Exponent diagram of system (5.1).*

Example 2. *Let us take the parameters* $n = 0.88, h = 1.15, s = 0.16, \alpha = 0.95, \delta = 0.6, r = 0.85, k = 1.33964$ *and the initial conditions* $x_0 = 0.54$ *and* $y_0 = 0.85$. *In this case, the system (1.3)*

experiences a Neimark–Sacker bifurcation. The eigenvalues of Jacobian matrix evaluated at unique positive coexistence fixed point $\vartheta_3 = (0.372787, 0.857596)$ *are* $\lambda_{1,2} = 0.971344 \mp 0.237677i$ *such that* $\left|\lambda_{1,2}\right| = 1$. *For* $\delta = 0.65, n = 0.88, h = 1.15, s = 0.16, \alpha = 0.95, r = 0.85, k = 1.33964$, *the system has a unique positive fixed point* $\vartheta_3 = (0.335641, 0.868625)$. *It is clear that* ϑ_3 *is unstable fixed point of system (1.3). In order to control the system (1.3) with OGY and feedback control methods, we take* $\delta_0 = 0.65$. *The controlled system dynamics are governed by*

$$\begin{aligned} x_{n+1} &= \frac{[1.33964\, x_n + 0.9775\, x_n(1.33964 - x_n)](1 + 0.88\, x_n)}{1.33964(1 + 0.88\, x_n + 1.0925\, y_n)}, \\ y_{n+1} &= y_n + 1.15\left(\frac{0.95[0.65 - \rho_1(x_n - 0.335641) - \rho_2(y_n - 0.868625)]x_n y_n}{1 + 0.88\, x_n} - 0.16\, y_n\right). \end{aligned} \tag{5.2}$$

We have

$$A = \begin{bmatrix} 0.955058 & -0.163384 \\ 0.367607 & 1 \end{bmatrix},\ B = \begin{bmatrix} 0 \\ 0.245888 \end{bmatrix}$$

and

$$C = [B : AB] = \begin{bmatrix} 0 & -0.0401742 \\ 0.245888 & 0.245888 \end{bmatrix}.$$

Since C *has a rank of* 2, *the system can be controlled. Thus, the* $A - BK$ *matrix of the controlled system (5.2) can be expressed as*

$$A - BK = \begin{bmatrix} 0.955058 & -0.163384 \\ 0.367607 - 0.245888\rho_1 & 1 - 0.245888\rho_2 \end{bmatrix}.$$

The marginal lines l_1, l_2, *and* l_3 *in Eqs (4.8)–(4.10) are obtained as*

$$\begin{aligned} l_1 &= 0.01512 - 0.040174\rho_1 - 0.234837\rho_2 = 0, \\ l_2 &= 0.0600609 - 0.040174\rho_1 + 0.0110506\rho_2 = 0, \end{aligned}$$

and

$$l_3 = -3.97018 + 0.040174\rho_1 + 0.480725\rho_2 = 0.$$

The marginal stability boundaries l_1, l_2, *and* l_3 *delineate a triangular stability region in the* $\rho_1\rho_2$*-plane. Figure 2(a) illustrates this stable domain for the controlled system (5.2). Also, it is seen from Figure 2(b) that population becomes stable for the value* (ρ_1, ρ_2) *selected from this stable region.*

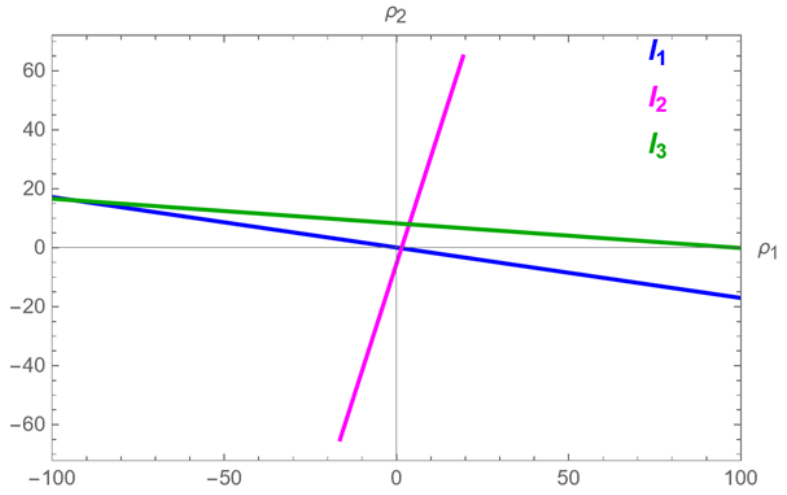

(a)

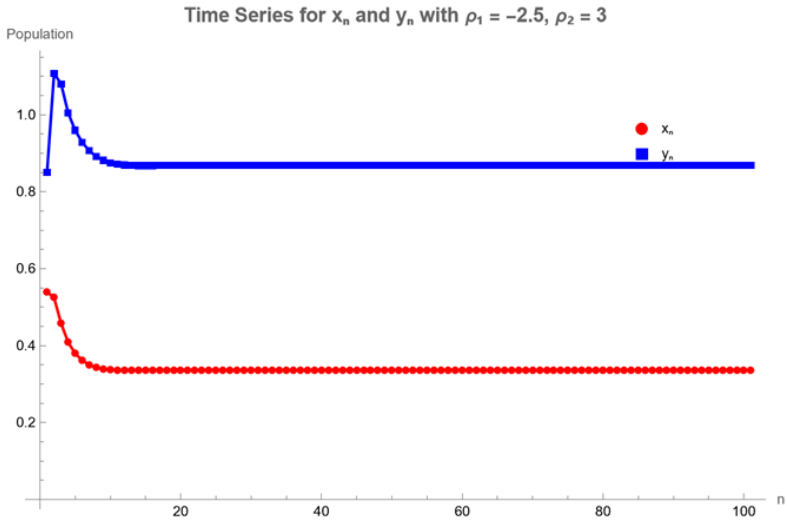

(b)

Figure 2. **(a)** Stability region for system (5.2) in the $\rho_1\rho_2$–plane. **(b)** The trajectories of the controlled system (5.2) in the $\rho_1\rho_2$–plane.

Example 2 demonstrates how a biologically unstable system can be dynamically regulated through appropriate control strategies to ensure ecological balance. Initially, for the given parameter values, the system exhibits a Neimark–Sacker bifurcation at the positive fixed point $\vartheta_3 = (0.372787, 0.857596)$, indicating the onset of quasiperiodic oscillations in prey and predator populations. Such behavior, if left uncontrolled, may correspond to persistent ecological fluctuations that destabilize coexistence. By applying the OGY method, the model transitions to a new fixed point, $\vartheta_3 = (0.335641, 0.868625)$, which becomes locally asymptotically stable. This intervention mimics real-world ecological management strategies, such as adaptive harvesting, prey inhibition, or environmental regulation, that seek to suppress population cycles and promote long-term species survival. The stability region depicted in the (ρ_1, ρ_2) parameter space (Figure 2(a),(b)) provides insight into the permissible ranges of control intensities needed to maintain ecological balance.

Example 3. *We again consider the parameters* $\delta = 0.6, n = 0.88, h = 1.15, s = 0.16, \alpha = 0.95, r = 0.85$ *with* $k = 1.4$ *and the initial conditions* $x_0 = 0.54$ *and* $y_0 = 0.85$. *For these parameter values, the controlled system is*

$$\begin{aligned} x_{n+1} &= \frac{[1.4x_n + 0.9775x_n(1.4 - x_n)](1 + 0.88x_n)}{1.4(1 + 0.88x_n + 1.0925y_n)} - \tau_1(x_n - \overline{x}) \\ &\quad - \tau_2(y_n - \overline{y}) \\ y_{n+1} &= y_n + 1.15(\frac{0.57x_ny_n}{1 + 0.88x_n} - 0.16y_n). \end{aligned} \tag{5.3}$$

Hence, there is a unique positive coexistence fixed point $(\overline{x}, \overline{y}) = (0.372787, 0.871853)$ *in the system (5.3). Furthermore, the Jacobian matrix calculated at* $(\overline{x}, \overline{y}) = (0.372787, 0.871853)$ *is*

$$\begin{bmatrix} 0.951596 - \tau_1 & -0.178584 - \tau_2] \\ 0.32403 & 1 \end{bmatrix}. \tag{5.4}$$

The marginal lines l_1, l_2, *and* l_3 *in Eqs (4.15)–(4.17) are obtained as*

$$\begin{aligned} L_1 &= -0.00946245 + \tau_1 - 0.32403\tau_2 = 0, \\ L_2 &= 0.0578665 + 0.32403\tau_2 = 0, \end{aligned}$$

and

$$L_3 = -3.96106 + 2\tau_1 - 0.32403\tau_2 = 0.$$

The stable triangular region in the $\tau_1\tau_2$*-plane is identified by the marginal lines* L_1, L_2, *and* L_3. *Figure 3(a) displays the area of the restricted system (5.3) bounded by these lines. Figure 3(b), the predator-prey populations are shown to quickly stabilize at constant values when* τ_1*=1.9 and* τ_2*=2.1.*

In Example 3, the predator-prey system is investigated under a different control parameter set, where $k = 1.4$, and the feedback gains τ_1 and τ_2 are introduced to stabilize the unique positive fixed point $(\bar{x}, \bar{y}) = (0.372787, 0.871853)$. This point represents a biologically meaningful steady-state where prey and predator coexist. From an ecological perspective, the application of feedback terms $\tau_1(x_n - \bar{x})$ and $\tau_2(y_n - \bar{y})$ mimics external regulation mechanisms, such as environmental interventions or adaptive behavior in population control. The calculated Jacobian matrix and corresponding stability boundaries delineate a triangular region in the (τ_1, τ_2)-plane where the system exhibits stable dynamics. This result emphasizes how small parameter adjustments in feedback control can restore ecological equilibrium and suppress oscillatory or unstable population cycles. The illustration in Figure 3(a),(b) further highlights the sensitivity of system stability to the feedback coefficients, offering insights into how ecological balance can be maintained through biologically plausible intervention strategies. The effectiveness of this strategy is not merely numerical; it reflects a fundamental ecological principle: *feedback-driven control can suppress instabilities and guide systems toward sustainable coexistence*, even in inherently unstable configurations.

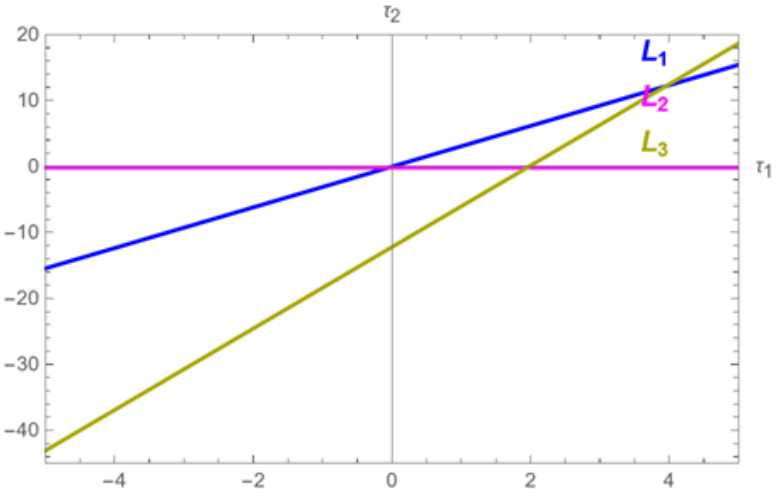

(a)

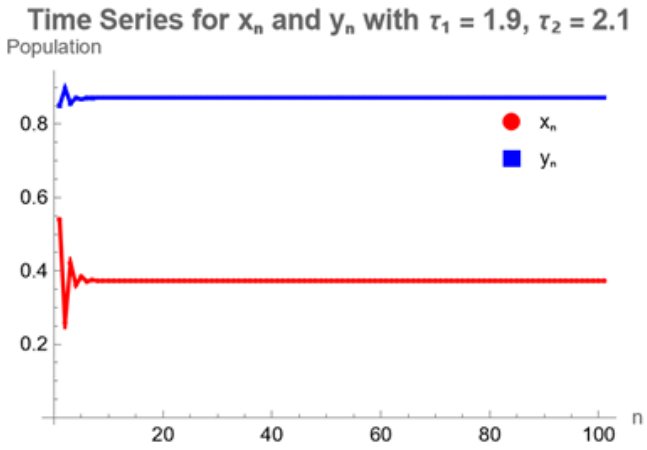

(b)

Figure 3. **(a)** Stability region for system (5.3) in the $\tau_1\tau_2$-plane. **(b)** The trajectories of the controlled system (5.3) in the $\tau_1\tau_2$-plane.

6. Conclusions

In this paper, the complex dynamic behavior of a discrete-time predator-prey system (1.3) is analyzed. The existence of fixed points of the system and their dynamics are examined. At the positive coexistence fixed point, we demonstrate the occurrence of a Neimark–Sacker bifurcation in the system. To avoid the chaos exhibited by the dynamic system, we use the OGY approach and state feedback method.

It is found that the system (1.3) possesses three fixed points: A coexistence positive fixed point ϑ_3, an exclusion fixed point ϑ_2, and a trivial (extinction) fixed point ϑ_1. It is clear that the system (1.3) has a unique positive coexistence fixed point $\vartheta_3 = (\frac{s}{\alpha\delta - ns}, \frac{r\delta(k(\alpha\delta - ns) - s)}{k(\alpha\delta - ns)^2})$ with $\alpha > \max\{\frac{ns}{\delta}, \frac{s(1+kn)}{\delta}\}$. Through

the use of mathematical methods related to bifurcation theory, we demonstrate that the system (1.3) undergoes Neimark–Sacker bifurcation when $k = \frac{\alpha\delta+s(n-hns+h\alpha\delta)}{(ns-\alpha\delta)(n(-1+hs)-h\alpha\delta)}$.

This study clearly demonstrates the potential of the nonstandard discrete model in ecosystem management by reconsidering the dynamic behavior of the predator-prey model presented with a different discretization scheme. The alternative nonstandard scheme implemented manages to capture both positive equilibrium conservation and Neimark–Sacker bifurcation values correctly. The suppression of chaos by various control strategies (OGY and state feedback) provides evidence for the manageability of complex behaviors in both theoretical and applied ecology. Our analysis shows that the bifurcation scenario remains unchanged and provides similar ecological insights despite the use of different nonstandard schemes. Moreover, the fact that management strategies that balance the ecosystem produce similar results strengthens our understanding of the model's internal dynamics.

The use of a NSFD scheme in this study ensures the preservation of ecologically relevant properties such as positivity and boundedness, which are essential when modeling population dynamics. This feature enhances the ecological relevance of the model, particularly in systems where discrete generational structure and species coexistence are critical. Moreover, the application of chaos control strategies, including the OGY method and state feedback control, demonstrates how theoretical tools can be used to stabilize ecological systems exhibiting unpredictable dynamics. Such approaches provide insight into how external interventions may help maintain ecological balance under fluctuating environmental conditions. Overall, this work contributes to the existing literature by combining NSFD-based modeling with bifurcation analysis and control techniques in a unified framework, offering both mathematical rigor and ecological applicability.

In [30], the continuous system undergoes a Hopf bifurcation near the positive equilibrium E_2 when the condition

$$\frac{s}{k(\delta\alpha - sn)} + \frac{\delta\alpha}{kn(\delta\alpha - sn)} = 1$$

is satisfied. Solving this expression for k using the values $n = 0.88$, $s = 0.16$, $\alpha = 0.95$, and $\delta = 0.6$ yields the critical bifurcation value $k \approx 1.8819$. In contrast, our discrete-time NSFD model with the same parameters exhibits a bifurcation at a significantly lower value, $k = 1.33964$, as shown in Example 6. This difference highlights that the discrete model may display bifurcation behavior at earlier stages compared to its continuous counterpart, revealing the enhanced sensitivity and richer dynamics captured by the NSFD scheme.

Although different formulations are adopted from [19] in the modeling process—such as using $x_n x_{n+1}$ instead of x_n^2, and $x_{n+1}y_n$ instead of $x_n y_n$—the Neimark–Sacker bifurcation threshold remains unchanged. Biologically, this indicates that the transition from stability to quasiperiodic oscillations is governed not by the specific timing of predator-prey interactions but rather by the structural balance of the model parameters. The use of time-lagged interactions better reflects realistic ecological processes such as delayed responses in reproduction, consumption, or adaptation. Yet, the persistence of the same bifurcation value under both modeling approaches suggests a form of ecological resilience: The critical dynamics of the system are preserved regardless of whether the interactions are synchronous or delayed by one time step. This underscores that population-level transitions, such as the onset of sustained oscillations, are deeply rooted in the nonlinear structure of the ecosystem, rather than in the discrete-time formulation details.

Use of Generative-AI tools declaration

The author declares she has not used Artificial Intelligence (AI) tools in the creation of this article.

Conflict of interest

The author declares no conflicts of interest in this paper.

References

1. A. A. Berryman, The origins and evolution of predator-prey theory, *Ecology*, **73** (1992), 1530–1535. https://doi.org/10.2307/1940005
2. R. M. May, *Stability and complexity in model ecosystems*, Princeton University Press, Princeton, NJ, USA, 1974. https://doi.org/10.1109/TSMC.1976.4309488
3. C. Köme, Y. Yazlık, Stability, bifurcation analysis and chaos control in a discrete predator-prey system incorporating prey immigration, *J. Appl. Math. Comput.*, **70** (2024), 5213–5247. https://doi.org/10.1007/s12190-024-02230-0
4. Ö. A. Gümüş, A study on stability, bifurcation analysis and chaos control of a discrete-time prey-predator system involving Allee effect, *J. Appl. Anal. Comput.*, **13** (2023), 3166–3194. https://doi.org/10.11948/20220532
5. Rajni, S. Sahu, S. Sarda, B. Ghosh, Stock patterns in a class of delayed discrete-time population models, *Discrete Contin. Dyn. Syst. Ser. S*, **18** (2025), 1285–1303. https://doi.org/10.3934/dcdss.2024078
6. Z. Eskandari, P. A. Naik, M. Yavuz, Dynamical behaviors of a discrete-time prey-predator model with harvesting effect on the predator, *J. Appl. Anal. Comput.*, **14** (2024), 283–297. https://doi.org/10.11948/20230212
7. Ö. A. Gümüş, Bifurcation analysis and chaos control of discrete-time prey-predator model with Allee effect, *Hacet. J. Math. Stat.*, **22** (2023), 1–17. https://doi.org/10.15672/hujms.1179682
8. M. Qurban, A. Khaliq, M. Saqib, T. Abdeljawad, Stability, bifurcation, and control: Modeling interaction of the predator-prey system with Allee effect, *Ain Shams Eng. J.*, **15** (2024), 102631. https://doi.org/10.1016/j.asej.2024.102631
9. Ö. A. Gümüş, M. Fečkan, Stability, Neimark–Sacker bifurcation and chaos control for a prey-predator system with harvesting effect on predator, *Miskolc Math. Notes*, **22** (2021), 663–679. https://doi.org/10.18514/MMN.2021.3450
10. B. Ghosh, S. Sarda, S. Sahu, Torus doubling route to chaos and chaos eradication in delayed discrete-time predator-prey models, *Math. Method. Appl. Sci.*, **45** (2022), 1–18. https://doi.org/10.1002/mma.8789
11. J. Wang, C. Lei, Complex dynamics of a nonlinear discrete predator-prey system with Allee effect, *Open Math.*, **22** (2024), 20240013. https://doi.org/10.1515/math-2024-0013
12. P. Baydemir, H. Merdan, Bifurcation analysis, chaos control, and FAST approach for the complex dynamics of a discrete-time predator-prey system with a weak Allee effect, *Chaos Soliton. Fract.*, **196** (2025), 116317. https://doi.org/10.1016/j.chaos.2025.116317

13. Ö. A. Gümüş, A. A. Elsadany, A. M. Yousef, H. N. Agiza, Theoretical and numerical bifurcation analysis in a prey-predator model with prey harvesting effort, *Int. J. Model. Simul. Sci. Comput.*, **15** (2024), 1–21. https://doi.org/10.1142/S1793962325500163
14. A. Lotka, *Elements of physical biology*, Williams and Wilkins Co., Baltimore, MD, USA, 1925.
15. V. Volterra, Variazioni e fluttuazioni del numero d'individui in specie animali conviventi, *Mem. R. Accad. Naz. Lincei*, **2** (1926), 31–113.
16. R. M. May, *Theoretical ecology: Principles and applications*, Blackwell Science, Oxford, 1976.
17. S. M. Moghadas, M. E. Alexander, B. D. Corbett, A non-standard numerical scheme for a generalized Gause-type predator-prey model, *Physica D*, **188** (2004), 134–151. https://doi.org/10.1016/S0167-2789(03)00285-9
18. W. Koa, K. Ryu, A qualitative study on general Gause-type predator-prey models with non-monotonic functional response, *Nonlinear Anal.-Real*, **10** (2009), 2558–2573. https://doi.org/10.1016/j.nonrwa.2008.05.012
19. A. Q. Khan, A. Maqbool, M. J. Uddin, S. M. S. Rana, Dynamical analysis of a two-dimensional discrete predator-prey model, *J. Comput. Appl. Math.*, **440** (2024), 115578. https://doi.org/10.1016/j.cam.2023.115578
20. H. I. Freedman, *Deterministic mathematical models in population ecology*, Marcel Dekker, New York, 1980.
21. S. M. S. Rana, Dynamic complexity in a discrete-time predator-prey system with Michaelis–Menten functional response: Gompertz growth of prey, *Comput. Ecol. Softw.*, **10** (2020), 117–132.
22. R. E. Kooij, A. Zegeling, Predator-prey models with non-analytical functional response, *Chaos Soliton. Fract.*, **123** (2019), 163–172. https://doi.org/10.1016/j.chaos.2019.03.036
23. Z. Eskandari, Z. Avazzadeh, R. K. Ghaziani, B. Li, Dynamics and bifurcations of a discrete-time Lotka–Volterra model using nonstandard finite difference discretization method, *Math. Method. Appl. Sci.*, **48** (2022), 7197–7212. https://doi.org/10.1002/mma.8859
24. L. J. Allen, *Introduction to mathematical biology*, Pearson/Prentice Hall, New Jersey, 2007.
25. J. D. Murray, *Mathematical biology: I. An introduction*, Springer, New York, 2002.
26. D. T. Dimitrov, H. V. Kojouharov, Nonstandard finite-difference methods for predator-prey models with general functional response, *Math. Comput. Simul.*, **78** (2008), 1–11. https://doi.org/10.1016/j.matcom.2007.05.001
27. Z. Iqbal, M. A. U. Rehman, M. Imran, N. Ahmed, U. Fatima, A. Akgul, et al., A finite difference scheme to solve a fractional order epidemic model of computer virus, *AIMS Math.*, **8** (2023), 2337–2359. https://doi.org/10.3934/math.2023121
28. G. F. Gause, *The struggle for existence*, Williams and Wilkins, Baltimore, 1934, 123–147. https://doi.org/10.5962/BHL.TITLE.4489
29. A. Martin, S. Ruan, Predator-prey models with delay and prey harvesting, *J. Math. Biol.*, **43** (2001), 247–267. https://doi.org/10.1007/s002850100095
30. A. B. Ashine, Global asymptotic stability analysis of predator-prey system, *Math. Model. Appl.*, **2** (2017), 40. https://doi.org/10.11648/j.mma.20170204.11

31. M. Peng, R. Lin, Z. Zhang, L. Huang, The dynamics of a delayed predator-prey model with square root functional response and stage structure, *Electron. Res. Arch.*, **32** (2024), 1–20. https://doi.org/10.3934/era.2024150
32. M. A. Khan, Q. Din, Codimension-two bifurcation in a class of a discrete-time predator-prey interaction with cannibalism, *Qual. Theor. Dyn. Syst.*, **24** (2025), 1–24. https://doi.org/10.1007/s12346-025-01235-9
33. W. Li, Q. Xu, X. Wang, C. Zhang, Dynamics analysis of spatiotemporal discrete predator-prey model based on coupled map lattices, *AIMS Math.*, **10** (2025), 1248–1299. https://doi.org/10.3934/math.2025059
34. R. E. Mickens, *Nonstandard finite difference model of differential equations*, World Scientific, Singapore, 1994.
35. R. E. Mickens, *Application of nonstandard finite difference schemes*, World Scientific, Singapore, 2000.
36. R. E. Mickens, Nonstandard finite difference schemes for differential equations, *J. Differ. Equ. Appl.*, **8** (2002), 823–847. https://doi.org/10.1080/1023619021000000807
37. Ö. A. Gümüş, Dynamic equilibria and bifurcation in predator and prey populations: A discrete-time approach, In: *14th Al Farabi Int. Sci. Res. Innov. Congr.*, Beyşehir, Türkiye, 2025, 864–873.
38. S. Elaydi, *An introduction to sifference equations*, Springer, New York, 1996.
39. M. R. S. Kulenović, G. Ladas, *Dynamics of second order rational difference equations: With open problems and conjectures*, Chapman and Hall/CRC, Boca Raton, 2001.
40. Y. A. Kuznetsov, *Elements of applied bifurcation theory*, Springer-Verlag, New York, 1998.
41. E. Ott, C. Grebogi, J. A. Yorke, Controlling chaos, *Phys. Rev. Lett.*, **64** (1990), 1196–1199. https://doi.org/10.1103/PhysRevLett.64.1196
42. C. Grebogi, Y. C. Lai, Controlling chaotic dynamical systems, *Syst. Control Lett.*, **31** (1997), 307–312. https://doi.org/10.1016/S0167-6911(97)00046-7
43. F. J. Romeiras, C. Grebogi, E. Ott, W. Dayawansa, Controlling chaotic dynamical systems, *Physica D*, **58** (1992), 165–192. https://doi.org/10.1016/0167-2789(92)90107-X
44. S. Lynch, *Dynamical systems with applications using mathematica*, Birkhäuser, Boston, 2007.
45. Q. Din, Bifurcation analysis and chaos control in discrete-time glycolysis models, *J. Math. Chem.*, **56** (2018), 904–931. https://doi.org/10.1007/s10910-017-0839-4
46. Q. Din, T. Donchev, D. Kolev, Stability, bifurcation analysis and chaos control in chlorine dioxide-iodine-malonic acid reaction, *MATCH Commun. Math. Comput. Chem.*, **79** (2018), 577–606.
47. S. Kapcak, Discrete dynamical systems with Sagemath, *Electron. J. Math. Technol.*, **12** (2018).

AIMS Press